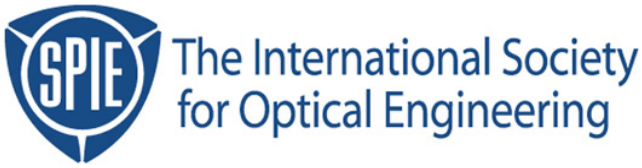

This paper was published in the proceedings of the
19th Annual BACUS Symposium on Photomask Technology and Management
SPIE Vol. 3873, pp. 189-202.
It is made available as an electronic reprint with permission of SPIE.

MEEF in Theory and Practice

F.M. Schellenberg[1] and Chris Mack[2]

[1]Mentor Graphics, 1001 Ridder Park Dr., San Jose, CA 95131
[2]FINLE Technologies, P.O. Box 162712, Austin TX 78716

ABSTRACT

The Mask Error Enhancement Function (MEEF) serves to amplify reticle errors. This can lead to proximity effects and bias problems that are much larger than would be expected from the normal reduction factor of the imaging system. The economic impact on reticle specifications can be severe. This paper examines the theoretical description of the MEEF for dark features: isolated lines, isolated posts, and dense 1:1 line/space features. MEEF for dense features is found in general to be smaller than 1 over a wide range, while MEEF for isolated features is always greater than 1. This "MEEF Gap" between isolated and dense features may help to explain the sensitivity of OPC to isolated and dense bias..

Keywords: MEEF, Mask Error Factor, MEF, Optical Lithography, OPC, Optical Proximity Correction.

1. INTRODUCTION

Moore's Law continues to drive developments in lithography to smaller and smaller dimensions [1][2]. Optical lithography at 180 nm using steppers with illumination at 248 nm wavelengths has now become routine, and for this sub-wavelength lithography domain, precise control of the reticle for Optical and Process Correction (OPC) has become critical. [3]

The existence of the Mask Error Enhancement Factor (MEEF) and its impact on lithography has been discussed for some time now [4][5][6][7]. This description is used to describe the relation between changes in the pattern found on the reticle and the corresponding pattern on the wafer. This is mathematically expressed as

$$MEEF = \frac{\partial CD_{wafer}}{\partial \left(CD_{reticle} / M \right)} \qquad \{1\}$$

where M is the imaging system reduction ratio (typically M=4 for DUV lithography systems). For an ideal linear imaging system, MEEF=1.0, which means that the reticle patterns correspond exactly to the reticle. In practice, process variables can significantly increase the MEEF as the image fidelity of the system deteriorates. [7]

Our intention with this paper is to review the behavior of the MEEF as it relates to the linearity behavior for three special dark features: Isolated lines, isolated posts, and dense line/space configurations.

2. CASE I: THE ISOLATED LINE

For an isolated line, shown in Figure 1, image linearity is a common metric for the quality of a lithography process. Typical linearity behavior for an isolated line is shown in Figure 2. The reticle, fabricated by DuPont Photomask and measured using a KLA-Tencor 8100-XP-R, shows excellent linearity – the reticle feature is almost exactly the target CD dimension, normalized for the reduction ratio M=4.

The image on the wafer, however, is significantly different. For larger features, the image formed on the wafer faithfully tracks the feature as produced on the reticle, but for linewidths significantly smaller than the wavelength used for lithography (in this case, 248 nm), the wafer CD begins to be significantly smaller than the target, until the process fails entirely and no measurable line is formed at all.

The nature of this behavior is easy to understand theoretically. For the simple 1-D line of width *a* (using 1X dimensions for notation convenience), the amplitude at the mask can be described by

$$M(x,y) = \begin{cases} 0, |x| < \dfrac{a}{2} \\ 1, |x| > \dfrac{a}{2} \end{cases} = 1 - \begin{cases} 1, |x| < \dfrac{a}{2} \\ 0, |x| > \dfrac{a}{2} \end{cases} = 1 - \prod\left(\frac{x}{a}\right) \qquad \{2\}$$

where we have used the notation of Bracewell for the Rectangle function Π(x) [8]. This is illustrated in Figure 3.

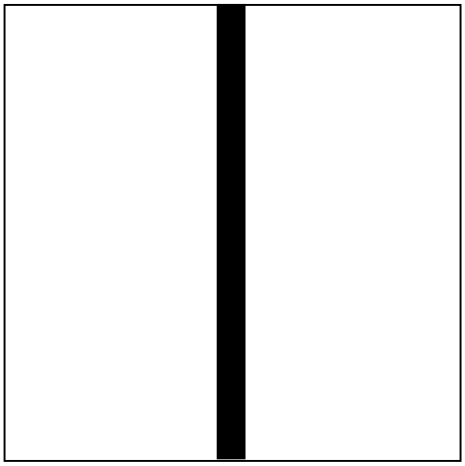

Figure 1: Illustration of the mask pattern for an isolated line

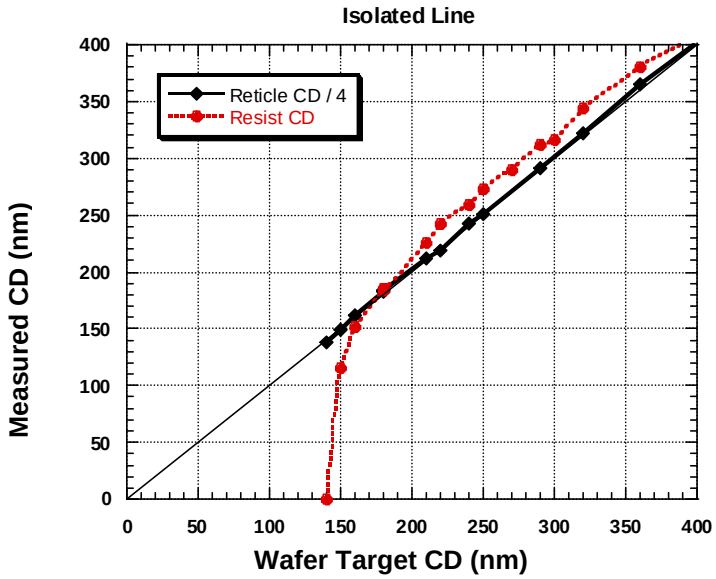

Figure 2: Measured linearity for an isolated dark line for a reticle (♦), and the corresponding wafer CD (•), measured in resist.

The behavior of an optical system can be reduced mathematically to a representation of the amplitude in the pupil plane [9]. In this case, for coherent illumination, the wavefront of the mask becomes the Fourier Transform of the mask function M(x,y). Because addition of Fourier Transforms is linear, and the transform of Π(x) is the well known sinc(ν), the transform becomes

$$F_M(\nu,\omega) = \delta(\omega)\left[\delta(\nu) - |a|\frac{\sin(a\pi\nu)}{(a\pi\nu)}\right] \qquad \{3\}$$

where ν represents the spatial frequencies in the x direction, and ω represents spatial frequencies in the y direction. This is illustrated in Figure 4. The coherent frequency cutoff of the of a circular pupil is given by ρ=NA/λ, where NA is the numerical aperture of the system, λ is the wavelength of light, and ρ is the radial spatial frequency

$$\rho = \sqrt{\nu^2 + \omega^2} \qquad \{4\}$$

The pattern at the pupil therefore becomes

$$F(\nu,\omega) = F_M(\nu,\omega) \times \prod\left(\frac{\rho\lambda}{2NA}\right) = \begin{cases} \delta(\omega)\left[\delta(\nu) - |a|\frac{\sin(a\pi\nu)}{(a\pi\nu)}\right] & |\nu| < \frac{NA}{\lambda} \\ 0 & |\nu| > \frac{NA}{\lambda} \end{cases} \qquad \{5\}$$

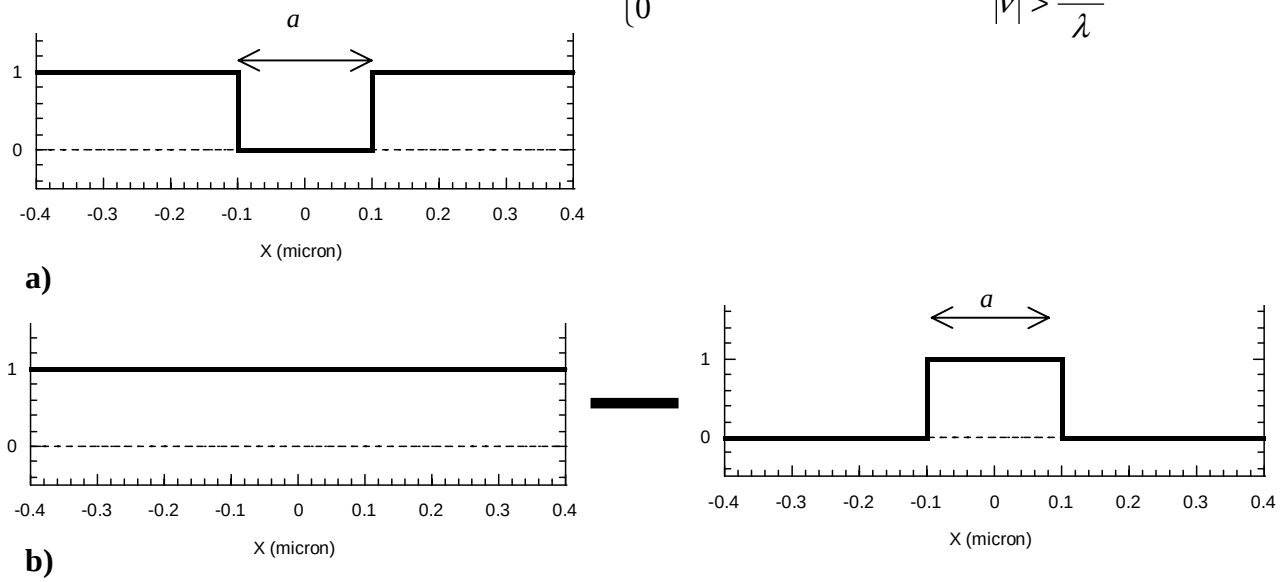

Figure 3: a) The original mask function for a isolated dark line of width *a*, in this case with *a*=0.2 micron, and b) the decomposition according to equation {2}.

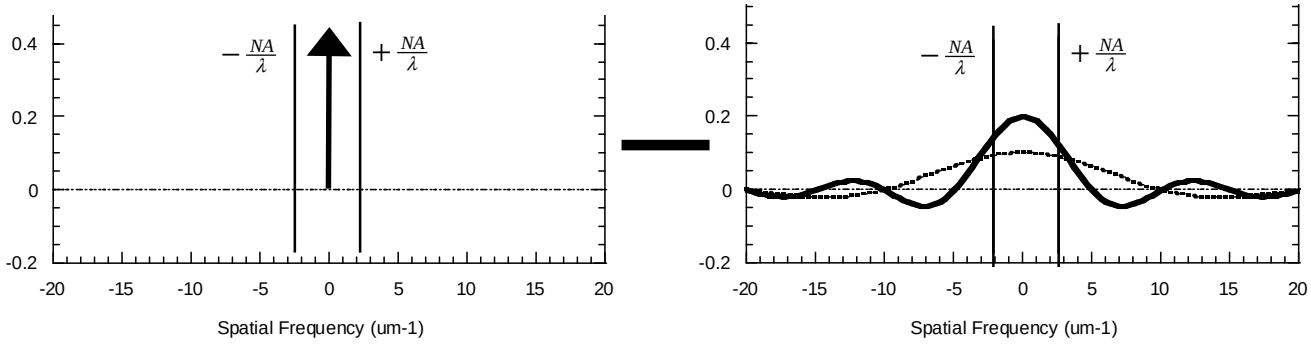

Figure 4: The frequency spectrum for functions of Figure 3, with frequency cutoff for NA=0.63 and λ=0.248 μm given by ν=2.54 μm^{-1}. The two curves plotted on the right correspond to *a*=0.20 μm (solid) and *a*=0.10 μm (dashed).

The inverse transform corresponding to the electric field at the image then becomes

$$E(x,y)=\left[1-\prod\left(\frac{x}{a}\right)\right]\otimes\left[\frac{2NA}{\lambda}\frac{\sin(2\pi xNA/\lambda)}{(2\pi xNA/\lambda)}\right] \quad \{6\}$$

where ⊗ represents convolution and the term on the right is the line-spread function. Because

$$\int_{-\infty}^{\infty}\mathrm{sinc}(u)du=1 \quad \{7\}$$

and, for small *a*, we can approximate

$$\prod\left(\frac{x}{a}\right)\approx a\delta(x) \quad \{8\}$$

the image field then becomes

$$E(x,y)\approx 1-a\left[\frac{2NA}{\lambda}\frac{\sin(2\pi xNA/\lambda)}{(2\pi xNA/\lambda)}\right] \quad \{9\}$$

The image intensity $I(x,y)=|E(x,y)|^2$ can be approximated by

$$I(x,y)\approx 1-2a\left[\frac{2NA}{\lambda}\frac{\sin(2\pi xNA/\lambda)}{(2\pi xNA/\lambda)}\right]+a^2\left[\frac{2NA}{\lambda}\frac{\sin(2\pi xNA/\lambda)}{(2\pi xNA/\lambda)}\right]^2 \quad \{10\}$$

This is illustrated in Figure 5. This essentially describes a bright field with the line spread function subtracted in proportion to the width of the isolated feature.

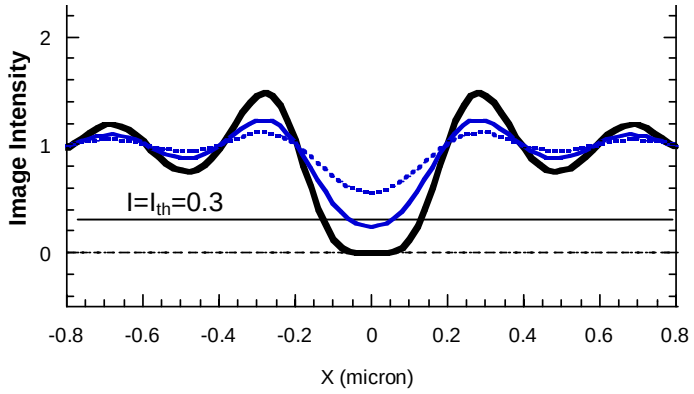

Figure 5: Coherent image formed according to Equation [x] for *a*=0.2 μm (thick solid), *a*=0.1 μm (light solid), and *a*=0.05 μm (dashed). The linewidth on the wafer can be estimated by taking a slice at Ith=0.3

The CD is found by taking a slice of the image at constant intensity value and finding the distance between the two values of x that solve equation {10} as a transcendental equation with $I(x,y) = I_{th}$. This yields a prediction for small *a*, as shown in Figure 6. It is clear that, the smaller the value of *a*, the smaller the width of the feature, until the image dramatically shrinks to a linewidth of 0 when $x_{plus}=x_{minus}=0$. Because sinc(0)=1, this yields

$$a = \frac{\lambda}{2NA}\left(1-\sqrt{I_{th}}\right) \qquad \{11\}$$

For typical values NA=0.63, λ=248 nm, and I_{th}=0.3, this absolute minimum printable feature (linewidth vanishingly small) is a line with *a*=89 nm (1X) on the mask. This is significantly smaller than that observed in practice, as was illustrated in Figure 2, where the actual linewidth drops to 0 when the target CD is 140 nm. This difference occurs due to process effects that occur when imaging in resists that are significantly thicker than the features being produced.

The MEEF in this case is quite predictable. A small change in the isolated line thickness simply creates an isolated line that is smaller or larger, and the behavior in this case is predicted by moving up or down the linearity curve. As the linearity fails completely as the line becomes too dim, the MEEF increases dramatically as the slope of the linearity curve grows. The MEEF is simply derived from the differences in the linearity curve.

Qualitatively, this explains the actual behavior well. However, quantitatively, the discrepancies are real and large as illustrated in Figure 7. In fact, the MEEF for isolated lines in practice never drops below a value of 1.0. This simply emphasizes the difference in behavior for actual photolthography processes when compared with imaging simulation, especially coherent imaging simulation.

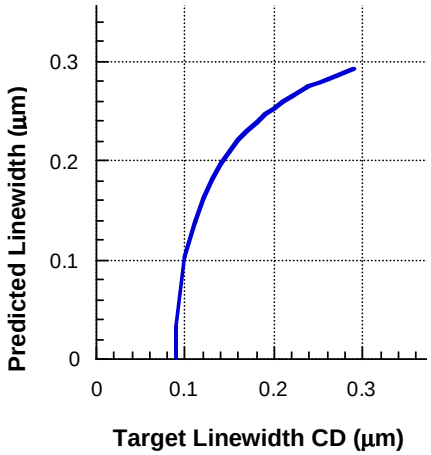

Figure 6: A plot of the linewidth predicted from curves for coherent images such as that shown in figure 5 for various values of 1X mask linewidth *a*. The approximations are valid only for small values of *a*.

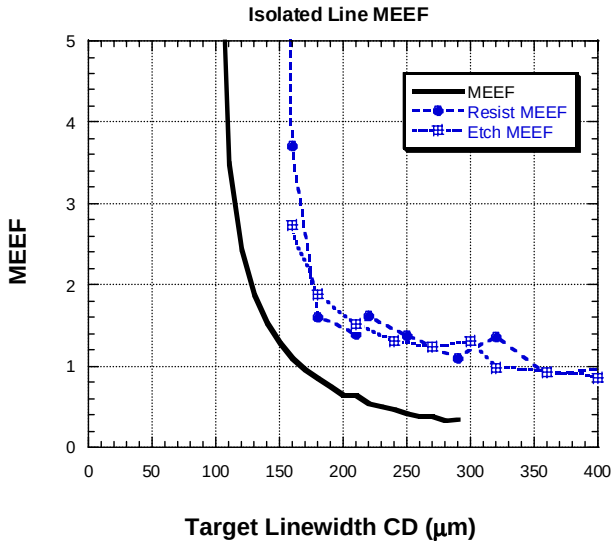

Figure 7: MEEF predicted using coherence theory (black) and data from processed silicon wafers. The theory leads to good qualitative understanding, but partial coherence effects and resist properties contribute significantly to the final measured MEEF.

2. CASE II: THE ISOLATED POST

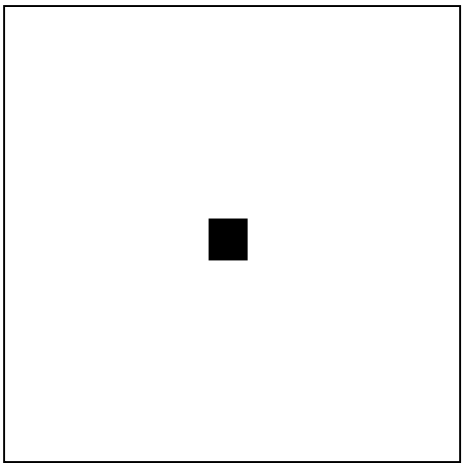

The case of the isolated post is very similar to that of the isolated line, with the exception that the mask is now defined by a two dimensional function

$$M(x,y) = 1 - \Pi\left(\frac{x}{a}\right)\Pi\left(\frac{y}{a}\right) \qquad \{12\}$$

This is illustrated in Figure 8. The Fourier pupil analysis yields an equation very similar to {3},

$$F_M(\nu,\omega) = \delta(\omega)\delta(\nu) - a^2 \frac{\sin(a\pi\nu)}{(a\pi\nu)} \frac{\sin(a\pi\omega)}{(a\pi\omega)} \qquad \{13\}$$

Figure 8: Illustration of the mask pattern for an isolated post.

This analysis is similar to the case of the isolated line, with truncation by a circular pupil of radius NA/λ, in a manner similar to equation {5} and {6} for the isolated line. However, now the mask function is fully two-dimensional, and the image of the filled pupil function is the Point Spread Function

$$PSF(r) = \frac{NA}{\lambda} \frac{J_1(2\pi r NA/\lambda)}{r} \qquad \{14\}$$

where $J_1(x)$ is the Bessel function of the first kind of order 1 [10]. The final image is therefore given by

$$E(x,y) \approx 1 - a^2 \frac{NA}{\lambda} \frac{J_1(2\pi r NA/\lambda)}{r} \qquad \{15\}$$

where $r=\sqrt{x^2 + y^2}$. When $I=I_{th}$, this becomes a transcendental equation which can be solved for r, just as was done in the case of the isolated line. Noting that $J_1(x)/x = 0.5$ when in the limit x=0, we can determine that the post vanishes when

$$a = \frac{\lambda}{NA}\sqrt{\frac{\left(1-\sqrt{I_{th}}\right)}{\pi}} \qquad \{16\}$$

For typical values NA=0.63, λ=248 nm, and I_{th}=0.3, this absolute minimum printable feature (i.e. post CD vanishingly small) is calculated to be a feature with *a*=149 nm (1X) on the mask. The rolloff behavior predicted by this would be qualitatively similar to that for the isolated line.

Figure 9 shows the experimental measurements of this rolloff for isolated posts in photoresist. Qualitatively, these are very similar to the isolated line, as predicted, but the point where the post fails is significantly larger than that for the isolated line (275 nm vs. 140 nm) and also significantly larger than would be predicted by this purely coherent imaging calculation.

A further complication is that the measurement taken from the reticle represents a 1-Dimensional CD, measured across the reticle feature. In fact, these features can be poorly formed, and the amount of light blocked by the post is significantly smaller than would be predicted by a rectangular post of the same CD dimension. This is similar to the case observed with contact holes in a previous paper [11].

The solution in that case was to substitute the actual CD as measured with an "effective" CD = √Area in the calculation of target dimension [ref us]. This makes the MEEF straightforward:

$$MEEF = \frac{\Delta CD_{wafer}}{\Delta "CD_{reticle}" / M} \qquad \{17\}$$

where "$CD_{effective}$" = √Area. Once the measured data for linearity is presented with this normalization, the MEEF is easily calculated again as the derivative of the linearity curve.

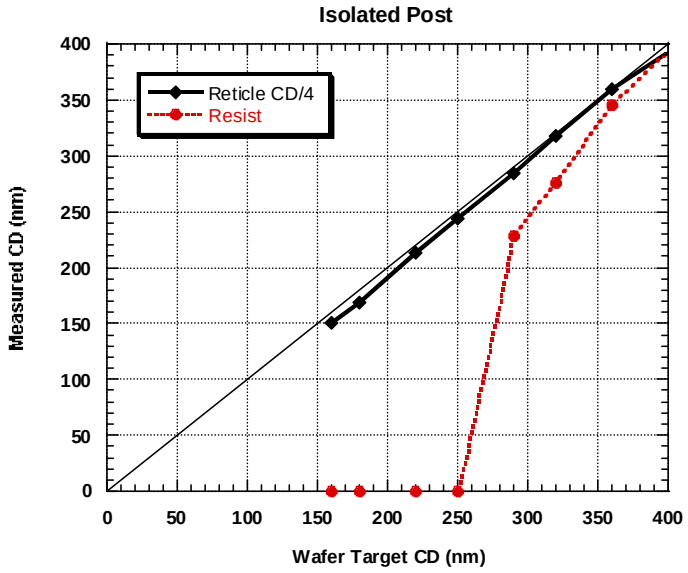

Figure 9: Measured linearity behavior for an isolated post. The deviation from linearity (MEEF > 1) begins for posts with a<350 nm, and fails completely for a<275 nm.

3. CASE III: EQUAL LINES AND SPACES

1. General Case

The case of equal lines and spaces, as illustrated in Figure 10, is not as straightforward. Although there are several measures for linearity that can be presented for dense lines, the most typical is the response of a constant 1:1 pitch as the spatial frequency changes. This would be parallel to the frequency response exemplified as the MTF for a classical optical system. Other measures commonly used to describe linearity of a different sort are pitch curves. These show linewidth changes that occur for features with constant nominal width as the pitch is changed from 1:1 to isolated. Although this has been a common analysis technique of interest for making predictions of OPC efficacy [12], the classic linearity curve shows the fundamental frequency response of the system, and will be the technique used here.

The mask function is defined by

$$M(x,y) = \left[\sum_{n=-\infty}^{n=\infty} \delta\left(\frac{x}{2a} - (n - 1/2)\right)\right] \otimes \prod\left(\frac{x}{a}\right) = \text{III}\left(\frac{x}{2a} + \frac{1}{2}\right) \otimes \prod\left(\frac{x}{a}\right) \qquad \{18\}$$

where a is the nominal linewidth and 2a is the pitch, and n is an integer. The notation for the replicating function III(x) is also from Bracewell [ref]. The corresponding Fourier spectrum is given by

$$F_M(\nu,\omega) = 2ae^{i2a\pi\nu}\text{III}(2a\nu) \times a\frac{\sin(a\pi\nu)}{a\pi\nu} \qquad \{19\}$$

This is illustrated in Figure 11. Note that the sign of the frequency components depends on the selection of origin. We have made the arbitrary selection of the center of a dark fringe as the origin in this example, making the mask function even and dictating that all frequency components are real and symmetric.

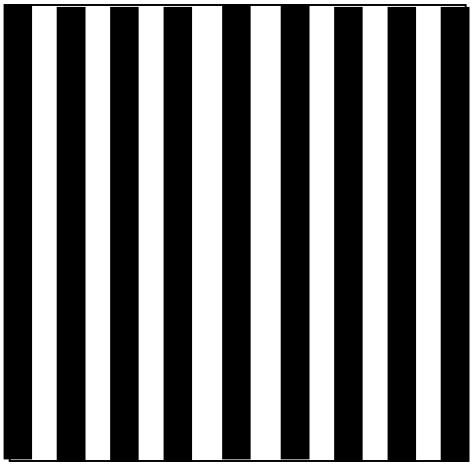

Figure 10: Illustration of the mask pattern for equal lines and spaces.

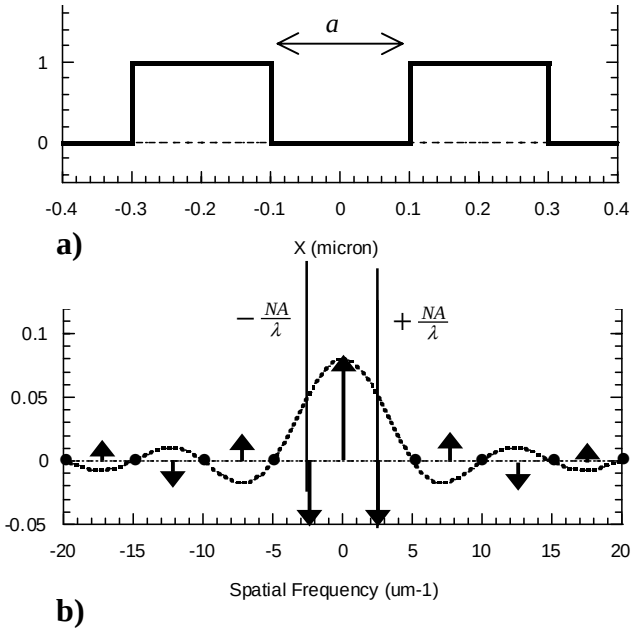

Figure 11 a) Mathematical description of equal lines and spaces for a=0.2, and b) the corresponding pupil function. Sign conventions are dictated by the symmetry choice illustrated in 11a).

Again, in this case, the frequency cutoff of the pupil truncates all but the first orders from being transmitted and recollected to form the image. The pupil function then becomes

$$F(\nu,\omega) = 2ae^{i2a\pi\nu}\frac{1}{2a}\left[\delta(\nu)+\delta\left(\nu-\frac{1}{2a}\right)+\delta\left(\nu+\frac{1}{2a}\right)\right]\times a\frac{\sin(a\pi\nu)}{a\pi\nu} \quad \{20a\}$$

$$= 2a^2\left[\frac{1}{2a}\delta(\nu)-\frac{1}{2a}\delta\left(\nu-\frac{1}{2a}\right)\frac{\sin(\pi/2)}{\pi/2}-\frac{1}{2a}\delta\left(\nu+\frac{1}{2a}\right)\frac{\sin(\pi/2)}{\pi/2}\right] \quad \{20b\}$$

$$= a\delta(\nu)-2a^2\frac{2}{\pi}\left[\frac{1}{2}\delta\left(a\nu-\frac{1}{2}\right)+\frac{1}{2}\delta\left(a\nu+\frac{1}{2}\right)\right] \quad \{20c\}$$

Note from Figure 11b that the coincidence of the periodicity being equal to twice the linewidth means that the only 3 major frequency components contribute to the final image. Furthermore, The term in brackets on the right is easily recognized as II(ν), the transform of cos(πx). The image therefore corresponds to a zero frequency background light component, modulated by the cosine term. The relative amplitudes are fixed, as can be seen from Figure 11.

Although providing good conceptual explanations, as we have seen, coherent imaging models are especially not very accurate when it comes to dense lines and spaces because the MTF of the lens, interacting with partial coherence, plays a significant role in defining the overall transmission of the various frequency components. We instead turn to partially coherent aerial image simulation for the rest of the paper, with a partial coherence factor σ=0.5.

The imaging behavior of equal line/spaces under these conditions and with λ=248 nm and NA = 0.63 is shown in Figure 12. The behavior for larger features is linear, as expected, but for features nearer to the frequency cutoff, the behavior takes a surprising upswing before totally collapsing. This represents the changing bias introduced by the zero frequency components of the spectrum, as the contrast of the image itself is reduced. All these simulations were generated using a constant intensity threshold value of 0.3. Selecting a slightly different value can change this upswing behavior.

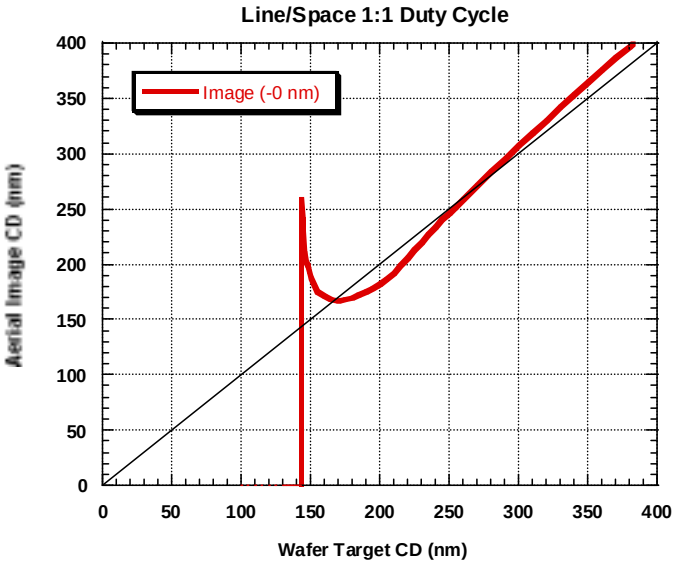

Figure 12: Plot of the CD as calculated from aerial image for dense Line/Spaces with a 1:1 Duty Cycle. The frequency response has a distinct upswing before completely collapsing at 150 nm.

To assume the derivative of this linearity curve is the MEEF would lead to very surprising behavior indeed. The slope of this linearity response curve is 0 for target CDs around 175 nm, and negative for values below this. A negative MEEF would imply that an increase in linewidth on the reticle could actually case a decrease in feature size, something that is not observed experimentally. Yet imaging in this regime is known in practice to have extreme sensitivity to mask errors and process conditions, and MEEF behavior is always positive. Clearly something other than the derivative of this linearity curve must be used to evaluate the MEEF.

The definition of MEEF as stated in equation {1} is correct, but we need to be careful about how we define CD. The analysis is similar to that carried out for isolated lines, there are two distinct types of changes on the reticle that can occur. The first is a global error, in the form of a feature bias that can arise from processing conditions. The other is a local error, or an error that occurs in a single line, either due to a writing error or a localized defect.

2. Case IIIa: Global bias

In the case of a global bias, all lines are uniformly distorted, either being wider or narrower than the target linewidth. An example for smaller lines is illustrated in Figure 13. The mask can be expressed mathematically as.

$$M(x,y) = \text{III}\left(\frac{x-a}{2a}\right) \otimes \prod\left(\frac{x}{a-d}\right) \qquad \{21\}$$

where d is the total change in the width of the target CD with the perturbation. This is illustrated in Figure 14a. For a thinner line. d has a positive value, while for a thicker line, d has a negative value.

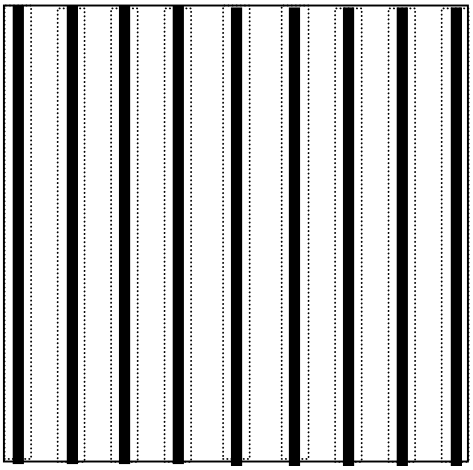

Figure 13: Illustration of the mask pattern for equal lines and spaces with a constant process bias.

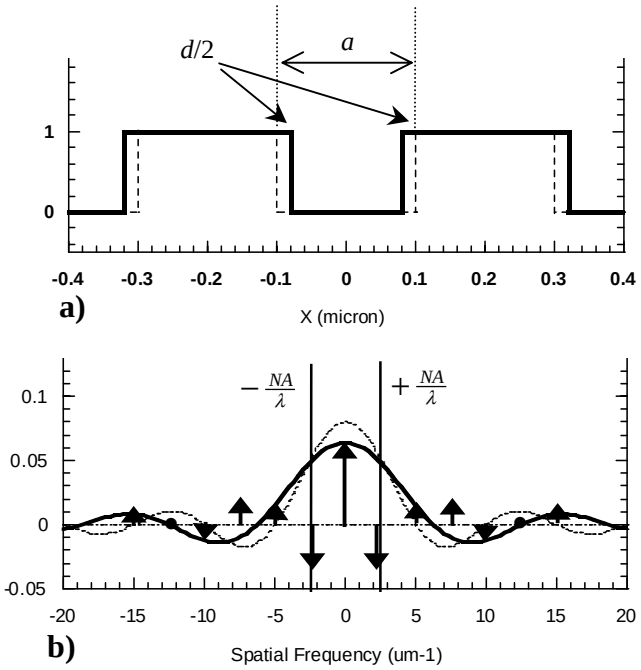

Figure 14 a) Mathematical description of equal lines and spaces for a=0.2 um, with a process bias of d=0.04 um, and b) the corresponding pupil function.

The pattern at the pupil is given by the Fourier Transform, which becomes

$$F_M(\nu,\omega) = 2ae^{-i2\pi\nu/2a}\,\text{III}(2a\nu) \times (a-d)\frac{\sin((a-d)\pi\nu)}{(a-d)\pi\nu} \qquad \{22\}$$

is illustrated in Figure 14b. In this case, the periodicity of the sampling function is still the same, but the narrower (wider) the feature itself, the wider (narrower) the corresponding sinc function in Fourier space. This breaks the degeneracy of the sampling points with the nulls in the sinc function. Although generally beyond the frequency cutoff for coherent light, for partially coherent illumination the second order diffracted light begins to pass through the pupil and contribute to the image contrast as well.

The effect this has on the linearity is shown in the simulations in Figure 15. As can be easily seen, the point of upswing changes somewhat with the width or narrowness of the line, moving to smaller feature sizes as more light passes through the mask (i.e. as the lines get thinner) until the upswing no longer occurs.

The MEEF is found by referring exactly to Equation {1}, and taking the difference between the curves of Figure 15 for corresponding spatial frequencies. The result is shown in Figure 16. This result is far more consistent with the experience of process engineers. Far from being the derivative of the linearity curve, the dense MEEF instead generally resembles the MEEF for isolated lines: near 1.0 for large features, rising catastrophically for features smaller than the wavelength.

Unlike the isolated lines, however, the MEEF is significantly less than 1 for a large range of spatial frequencies, in this case from 200 to 400 nm. The minimum MEEF is actually 0.7 when the feature size is slightly larger than the wavelength used in this particular example (248 nm). For comparison, as was shown in Figure 7, the MEEF for isolated lines is greater than 1 over this range, and never less than 1 in any circumstance.

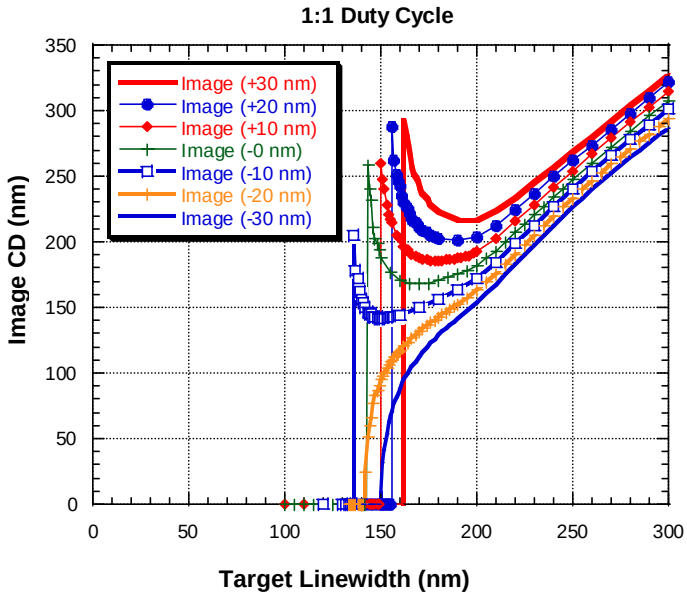

Figure 15: Image linewidths for "equal" lines and spaces, using a variety of values for the process bias d.

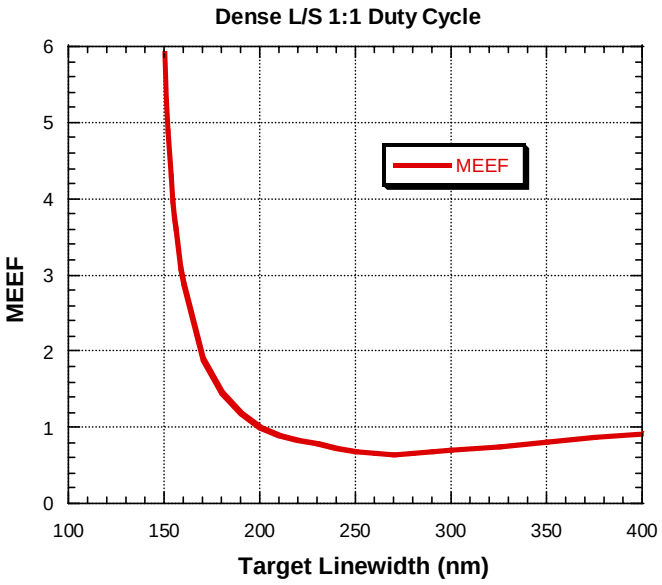

Figure 16: MEEF for the dense lines calculated in Figure 15. The value clearly drops below 1 for a wide range of target CD values.

3. Case IIIa: The Effect of Photoresist.

All the simulations of dense lines so far used aerial image simulation with a conventional threshold value of 0.3. When exposure and processing parameters are taken into account, process simulation can be used to estimate these effects. The mask design used for linearity measurements of isolated features did not have this particular set of dense perturbations on it, so the equivalent results must be generated through simulation. A software tool like PROLITH/3D provides well calibrated models of resist and processing effects for this purpose.[13]

All the simulations for isolated lines so far used aerial Using the resist parameters listed in Table I, PROLITH/3D simulations were carried out for the case outlined above, and the corresponding MEEF calculated. The result is illustrated in Figure 17. Qualitatively, the MEEF follows the same behavior, being near 1 for large features, shrinking to 0.7 for features slightly larger than the wavelength, and rising catastrophically as the feature size is smaller than the wavelength. However, this rise occurs sooner than in the pure aerial image case, just as was observed in the isolated case.

The final comparison between isolated and dense MEEF under process conditions is shown in Figure 18. The line is drawn as a guide to the eye through the array of measured datapoints that were plotted in Figure 7. The "MEEF Gap" ranging from 200 to 400 nm is clear, and as large as 0.6 at maximum separation. This difference calls for better characterization of MEEF not just for isolated lines, but for both isolated and dense lines, and the need to anticipate this susceptibility to errors in making OPC.

This might explain the relative lack of difficulty with mask specification and manufacturing that makers of dense chips with a high degree of periodicity (such as DRAMs) often encounter in subwavelength lithography, compared to the greater difficulty encountered in designs (such as ASICs) that have a wide range of isolated and dense features. This iso-dense MEEF difference may be the real reason iso-dense bias effects are so significant for OPC – not only can a bias exist, but the ability to correct isolated features is made more difficult due to the differences in MEEF.

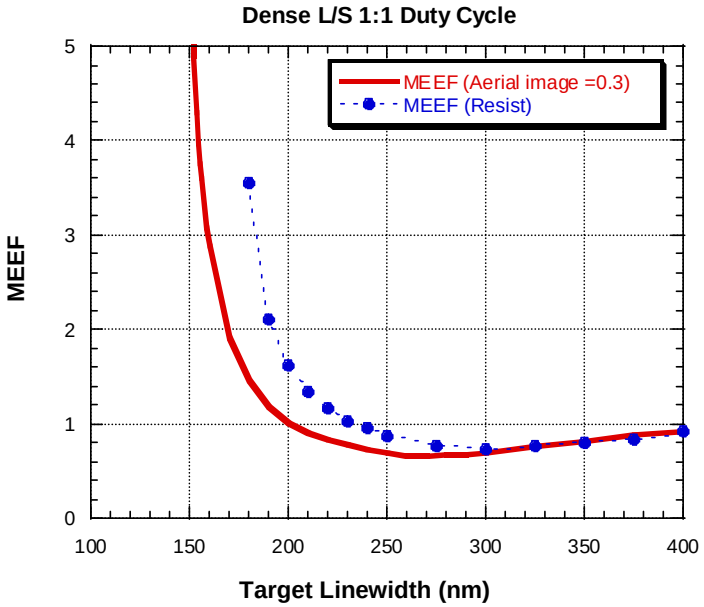

Figure 17: Plot of the MEEF as calculated for dense 1:1 line/space pairs using aerial image as well as full resist processing parameters.

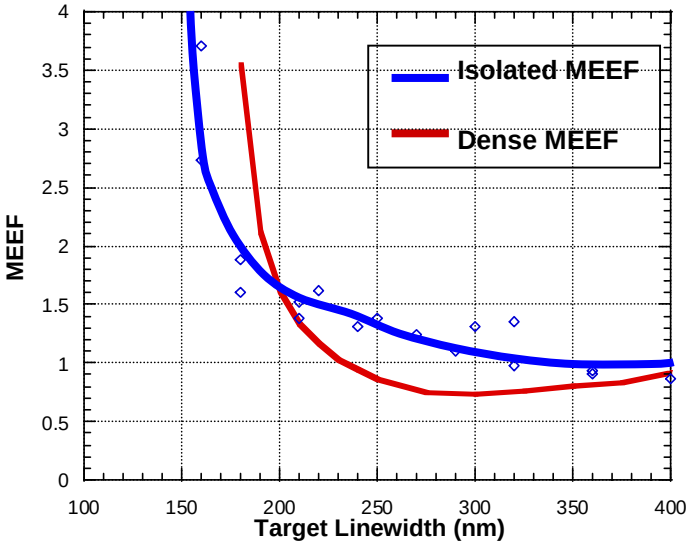

Figure 18: Plot of MEEF in photoresist, measured for isolated lines and calculated for dense lines. There is a pronounced "MEEF Gap" centered around 275 nm where the difference in MEEF can be as large as 0.6.

Table I:
PROLITH Resist Simulation Parameters

Stepper:
λ=0.248 nm NA=0.63 σ=0.5

Film Stack
UV6 resist (600 nm) with DUV18 ARC (180 nm)

Dose:
13.2 mJ/cm2

Post-Exposure Bake
90 sec at 125° C

Development Time
60 sec.

4. Case IIIb: An isolated Defect

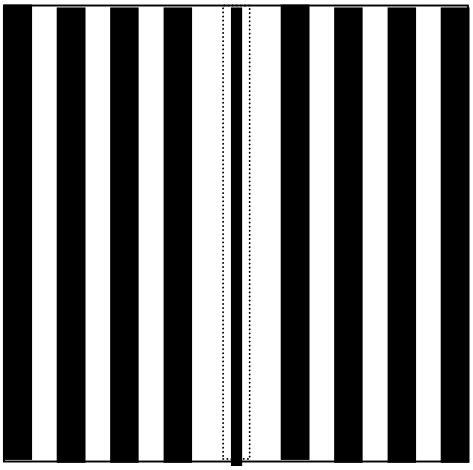

Figure 19: Illustration of the mask pattern for equal lines and spaces with an error in a single feature.

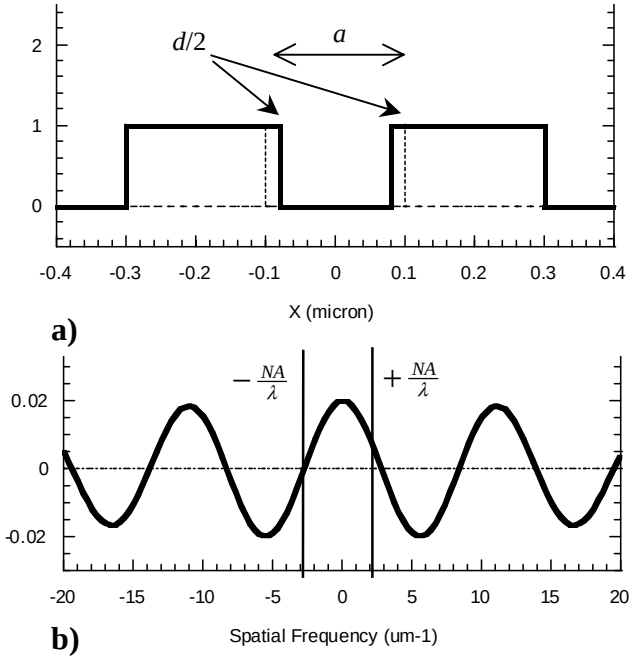

Figure 20 a) Mathematical description of equal lines and spaces for a=0.2 um, with a process bias of d=0.04 um for the center line, and b) the corresponding frequency spectrum for the defect.

For completeness, we mention one other possible defect but will not do the full analysis here. In this case, only the center line of the defect grows or shrinks. This is illustrated in Figure 19. The Mask function is no longer periodic, but is given by

$$M(x,y) = \text{III}\left(\frac{x-a}{2a}\right) \otimes \prod\left(\frac{x}{a}\right) + \prod\left(\frac{x-(a/2-d/4)}{d/2}\right) + \prod\left(\frac{x+(a/2-d/4)}{d/2}\right) \qquad \{23\}$$

where d is the total change in CD with the perturbation, as illustrated in Figure 20a. For a thinner line. d has a positive value, while for a thicker line, d has a negative value. The pattern at the pupil is given by the Fourier Transform, which becomes

$$F_M(\nu,\omega) = 2ae^{-i2\pi\nu a}\text{III}(2a\nu) \times (a)\frac{\sin(a\pi\nu)}{a\pi\nu} + \frac{d}{2}\frac{\sin(\pi d\nu/2)}{\pi d\nu/2}\cos\left(\pi\nu d\left(\frac{a}{d}-\frac{1}{2}\right)\right) \qquad \{24\}$$

The left portion of this is the unperturbed spectrum, as was plotted in Figure 11, while the right portion is the spectrum of the defect. This is plotted in Figure 20b).

The amplitude of this defect spectrum is much smaller than the spectrum plotted in Figure 11, suggesting that for d to be contributing significantly to this lithography, it would have to be very large. Furthermore, the MEEF will not be symmetric – larger features will tend to cause bridging, afecting neighboring features, while small features will simply tend to disappear. The analysis of these cross terms may require further analysis, and is beyond the scope of this work.

4. CONCLUSIONS

MEEF represents a significant problem for advanced lithography, and tools to better measure and characterize it are required. Estimates of the MEEF using coherent optical theory can provide some insight into the qualitative behavior, but any kind of quantitative prediction requires the use not only of aerial image, but simulation of the resist properties as well. We have also observed that the MEEF for isolated dark lines and dense 1:1 line/space pairs can be quite different, with a "MEEF Gap" as large as 0.6 forming between the two. This difference in susceptibility to mask errors may explain why MEEF has not been nearly as large a problem for DRAM manufacturers as it can be for ASICS, and may amplify the existing problem of isolated-dense bias.

5. ACKNOWLEDGEMENTS

The authors would like to thank Olivier Toublan of Mentor Graphics, Ed Charrier of FINLE Technologies Wilhelm Maurer of Infineorn, John Randall of Texas Instruments, and David Levenson of Pennwell Publications for helpful presentations and discussions; Craig West of DuPont Photomask and Franklin Kalk of the RTC for provisding the reticle used for these measurements; and Waiman Ng and Geoffrey Anderson of KLA-Tencor for providing the SEM metrology time.

6. REFERENCES

[1] Gordon E. Moore, "Lithography and the future of Moore's law", in Optical/Laser Microlithography VIII, Timothy A. Brunner; Ed., **Proc. SPIE Vol. 2440**, pp. 2-17 (1995).

[2] The National Technology Roadmap for Semiconductors, 1997 Edition (Semiconductor Industry Association, San Jose, 1997)

[3] F.M. Schellenberg, H. Zhang, and J. Morrow, "SEMATECH J111 Project: OPC Validation" in Optical Microlithography XI, Luc Van den hove, ed. **Proc. SPIE Vol. 3334**, pp 892-911, (1998)

[4] O. Toublan, D. Boutin, E. Luce, and P. Schiavone, "CD Dispersion and proximity bias across the lens field characterization by electrical linewidth measurement", in Proceedings of Interface '98 Conference (1998).

[5] W. Maurer and D. Samuels, "Masks for 0.25-micron lithography", in Photomask and X-Ray Mask Technology, HideoYoshihara; Ed. **Proc. SPIE Vol. 2254**, (1994), p. 26-35.

[6] W. Maurer, "Mask specifications for 193 nm lithography", in 16th Annual BACUS Symposium on Photomask Technology and Management, G.V. Shelden and J.A. Reynolds, Eds. **Proc SPIE Vol. 2884**, (1996), pp. 562-571.

[7] C. Mack, "Mask linearity and the mask error enhancement factor", **Microlithography World,** Winter 1999 p. 11-12.

[8] Ronald Bracewell, The Fourier Transform and its Applications, 2nd Edition, (McGraw hill, San Francisco, 1978).

[9] Joseph Goodman, Introduction to Fourier Optics (McGraw Hill, San Francisco, 1968).

[10] F.W.J. Olver, "Bessel Functions of Integer Order", ch. 9 of Handbook of Mathematical Functions (NBS Applied Mathematics Series 55), M. Abramowitz and I.A. Stegun, Eds. (U.S. Government Printing Office, Washington DC, 10th printing 1970).

[11] F.M. Schellenberg, V. Boksha, N. Cobb, J.C. Lai, C.H. Chen, and C.A. Mack, "Impact of mask errors on full chip error budgets" in Optical Microlithography XII, Luc Van den Hove; Ed, **Proc. SPIE Vol. 3679**, p. 261-275 (1999).

[12] J. Randall and A. Tritchkov, "Optically induced mask critical dimension error magnification in 248 nm lithography", **J. Vac. Sci. Technol. B16** , pp. 3606-3611 (1998).

[13] PROLITH is a product of FINLE Technologies; see C. Mack, Inside PROLITH: A Comprehensive Guide to Optical Lithography Simulation, (FINLE Technologies, Austin, TX 1997).